A multi-level data-driven Bayesian approach for stochastic model updating of complex aeroelastic systems

M. McGurk*
Aerospace Centre of Excellence, University of Strathclyde, Glasgow, UK, G1 1XJ

J. Yuan†
Computational Engineering Design Group, University of Southampton, Southampton, UK

The objective of this work is to propose a multilevel data-driven Bayesian framework to minimise the sampling requirement for stochastic model identification of general nonlinear aeroelastic systems. Adaptive Kriging based surrogate models are developed through multi-level Bayesian modeling updating to represent limit cycle oscillation (LCO) response of the nonlinear aeroelastic model. The proposed methodology is demonstrated on an aerofoil wing flutter model together with LCO experimental testing data. The results is benchmarked by the counterpart from a classical single-level approach. It is observed that the proposed approach offered a 74% reduction in training data requirement/run time and 3% accuracy improvement for the surrogate model.

I. Introduction

Utilising lightweight materials and incorporating electric propulsion systems is deemed essential for improving the efficiency and capabilities of aerospace systems. Modeling the dynamic response of lightweight aerospace structures poses a challenge due to their substantial geometric deformation. This deformation introduces distributed nonlinearities into structures, leading to intricate nonlinear dynamic behaviour [1, 2].

Nonlinearities in aeroelastic systems can result in subcritical post-flutter responses, leading to self-sustaining oscillations known as Limit Cycle Oscillations (LCO) at velocities below the linear flutter threshold [3, 4]. Experimental evidence of these behaviors has been observed in high-aspect-ratio flexible wings [5, 6], and recent studies have identified subcritical LCO formation in highly flexible wings during low-speed flutter experiments [7, 8]. Despite the importance of these nonlinear effects, they are often neglected in computational analyses due to complexity and high computational costs, limiting the design space for aerospace systems. Bifurcation diagrams describing LCO behavior are computationally expensive, and even with methods like harmonic balance continuation, computational efficiency remains a challenge, especially in high-fidelity systems [9]. Validating mathematical models that accurately capture system nonlinear responses is critical, as LCO identified through nonlinear analysis may pose structural risks in real systems. Reliable mathematical models could reduce the need for costly experiments under various flow conditions for certification.

Model updating is widely used to calibrate the parameters of mathematical or computation models based on experimental data in the last few decades [10, 11]. Most conventional techniques, including Least Squares minimization, Sensitivity-based model updating, and the Levenberg-Marquardt algorithm [12–14], offer deterministic parameter estimates. While these methods excel in linear systems, they prove computationally expensive and sensitive to noise in experimental data when applied to complex and high-dimensional dynamical systems [15]. Bayesian Model Updating (BMU), first put forward in [16], is regarded as one of the most promising probabilistic nonlinear parameter estimation techniques [17–19]. A significant advantage of BMU when compared to other probabilistic model updating techniques, such as Maximum Likelihood Estimation, is its capacity to seamlessly integrate prior knowledge [20].

In previous work a probabilistic data-driven methodology to minimise computational burden and maximise accuracy in identifying nonlinear models to capture LCO behaviour of aeroelastic systems was proposed [21]. Kriging models are developed with databases generated from nonlinear aeroelastic systems using harmonic balance method-based bifurcation analysis. LCO experimental data is obtained from a uniform wing test rig using control-based continuation testing methods [22]. Bayseian inference is then implemented between a Kriging surrogate model and experimental data to both estimate probabilistic parameters of the nonlinear model and rank the evidence supporting model selection. The

*PhD Candidate, Aerospace Centre of Excellence, michael.mcgurk@strath.ac.uk
†Corresponding author, Assistant Professor, Computational Engineering Design Group, j.yuan@soton.ac.uk

method offered an improvement on accuracy compared to deterministic approaches. An improvement in computational efficiency was also observed for forward uncertainty quantification. Lacking however, is interaction between the surrogate model was model updating.

This work proposes to improve computational efficiency further through an adaptive multi-level approach, implementing development of surrogate models within Bayesian model updating (BMU). As opposed to constructing a single accurate surrogate model then performing Bayesian inference, posterior distributions obtained with low fidelity surrogate models are used to build refined surrogate models. This process is repeated in levels until a converged solution is reached.

Building reduced order models through multi-level approaches has become common in engineering design [23–25]. Bayesian model updating has been used to assist in building reduced order models such as in [26] where prior distributions define a reduced design space to construct reduced order models. In [27] the inverse is carried out, where BMU was implemented to estimate parameters based on a data-driven reduced order model. Dodwell and co present a method where reduced amounts of data is used to construct a coarse update of model through Baysiean inference [28, 29]. This is repeated in levels until a stationary posterior distribution is reached. Through this method, the number of times the potentially cost model is ran is reduced by up to three times compared to single-level approaches. The methodology proposed in this work combines the concepts discussed here. While individual steps are not unique, the way they are combined is novel. The leveled approach to model updating from [28, 29] is applied but fidelity of surrogate model is not updated each level as opposed to amount of evidence data. As in [29] the prior distribution from BMU is used to define the space the data-driven model is refined to.

This paper will present an adaptive data-driven approach through multi-level BMU and discuss how it differs from the single-level approach in [21]. The nonlinear aeroelastic case study is then presented with experimental dated and mathematical model. A reference study is then carried out using the single-level approach before applying the multi-fidelity methodology to the case study. The sets of results are compared and benefits of each method discussed. The main goal of the paper is to demonstrate, the number computationally expensive continuation runs can be reduced in the multi-fidelity approach compared to the single level process.

II. Methodology

In this section, the principle of Bayesian model updating will be described as it is integral to understanding both single- and multilevel data driven updating. The single-level updating process will then be presented, before the multi-level method is laid out.

A. Bayesian model updating

The Bayesian interface is implemented to estimate posterior distributions of nonlinear parameters from a prior distribution using input data and a likelihood function including experimental data. Posterior distributions of parameters θ are estimated with:

$$P\left(\theta|\mathbf{V}\right) = \frac{P\left(\mathbf{V}|\theta\right).P\left(\theta\right)}{P\left(\mathbf{V}\right)} \tag{1}$$

where $\mathbf{V}$ is the vector of experimental points. The prior distribution is represented by $P(\theta)$, $P(\mathbf{V}|\theta)$ is the likelihood function, $P(\mathbf{V})$ is the evidence function and $P\left(\theta|\mathbf{V}\right)$ is the posterior distribution. The evidence function acts as a normalising constant to ensure the posterior integrates to one. Prior distributions reflect prior knowledge of the model parameters from observations.

The likelihood function reflects the degree of agreement between obtained measurements $\mathbf{V}$ and the output of model $f(\theta)$. Choice of likelihood function is dependent on the UQ metric. Assuming the error between observations and the model follows a zero mean normal distribution, a maximum likelihood estimation function is implemented as follows

$$P\left(\mathbf{V}|\theta\right) = \left(\prod_{i=1}^{n} \frac{1}{\sigma_i\sqrt{2\pi}}\right) \exp\left[-\sum_{i=1}^{n} \frac{\left(V_i - f\left(\theta^{(i)}\right)\right)^2}{2\sigma_i^2}\right] \tag{2}$$

Where σ_i is the variance of error between model and evidence. Equation 1 is evaluated by drawing samples from prior distributions until converged mean posteriors are reached. As the goal of the sampling is to converge to an unknown stationary distribution, standard methods (such as Monte-Carlo sampling) are not suited. Advanced sampling techniques are therefore employed commonly for optimal efficiency[30]. Transitional Chain Monte Carlo (TMCMC) sampling is implemented for this study based on the conclusions from previous study [21]. At the core of TMCMC, samples are

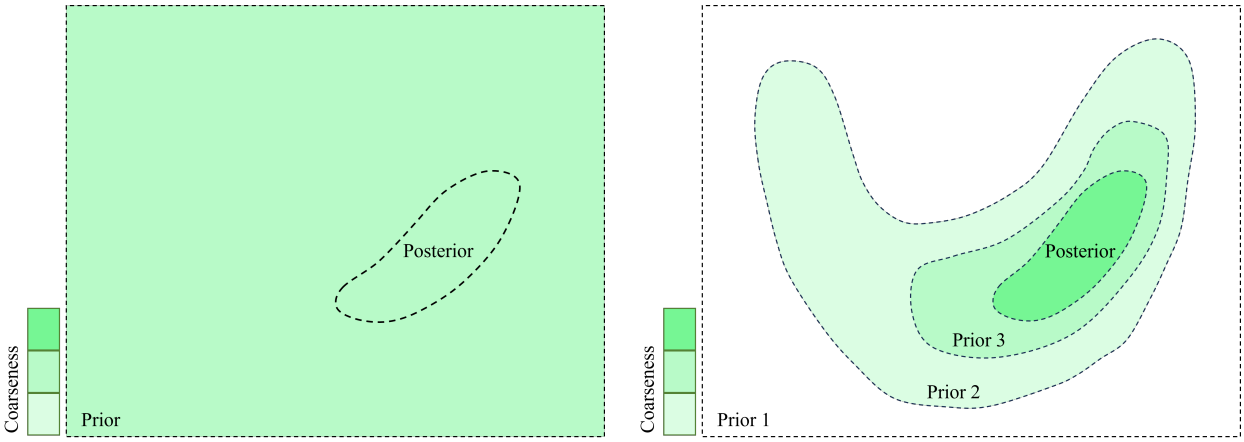

(a) Single level **(b) Multilevel**

Fig. 1 Data-driven model updating process

drawn based on a proposal distribution. They are either accepted or rejected depending on if they are within the prior distribution. An acceptance rate of between 0.15 to 0.5 with an optimal value of 0.234 ensures the design space is efficiently explored [31]. A Normal distribution is the common choice for the proposal, with the mean based around current sample θ_i and standard deviation σ_p that serves are the tuning parameter of the algorithm. Optimal σ_p (width parameter) is tuned until an acceptance rate as close to 0.234 is reached [32].

B. Single-level updating

Figure 1a describes the concept of single-level updating whereby a single data-driven model is built covering a full design space. Accuracy of the model is estimated based on mean comparison with a separate set of comparison data. Once accuracy of the model has converged to an acceptable degree, Bayesian model updating (BMU) is applied with the same prior distribution used to gather training data for the data-driven model. Algorithm 1 gives specific detail on estimating probabilistic response of high fidelity model f with data driven single-level updating. Inputs for unknown parameters θ are gathered with Latin Hypercube sampling (LHS) and then ran through the high fidelity model. Output data $\mathbf{Y}$ and corresponding input $\mathbf{X}$ are fed into a training algorithm $Train$ to produce the data-driven model. Convergence criterion for data-driven models a is based on the percentage difference in accuracy between data-driven models with increasing amounts of training data. As the single model required in the single-level process is required to have as high as possible accuracy, the convergence criterion is set high. Once accuracy of the model has converged BMU is utilised to estimate θ. With probabilistic estimates of θ, probabilistic response data $\mathbf{\Theta}$ can be obtained with the data-driven model and Monte-Carlo simulations (MCS) from the posterior distribution.

C. Multilevel updating

The multi-level approach is introduced with two goals (1) to reduce the amount of training data (2) to improve the accuracy of the converged data-driven model compared to the single-level process. Figure 1b presents the concept. Model updating is carried out with coarse models and the resulting prior distribution is used to gather training data for a less coarse data-driven model specialised to a reduced design space. Width parameter σ_p of the proposal distribution is reduced at each level converging with the estimate that would be used in the single-level process. In the current algorithm it is reduced by a factor related the the total number of levels and the current level. With larger width parameters at higher levels, the algorithm is able to explore more of the parameter space with coarse models. A detailed description of the process is presented in Algorithm 2. The key different with single-level updating is the presence of the a feedback loop over a set number of levels. At each level σ_p is reduced starting from $N_{level} \times \sigma_p$ until σ_p is reached at the final level. In the multilevel process, relative convergence criterion for data-driven models should be made lower than for the single-level process. This allows for initial coarse models to be developed with minimal training data. When constructing data-driven models after level 1, training points that were gathered for the previous layer that fall within the design space of the new prior distribution are held on to and those that fall outwith are discarded.

Algorithm 1 Single-level data-driven BMU

Input: Experimental data $\mathbf{V}$, Prior distribution $P(\theta)$, Width parameter σ_p, Training data increment inc_0, Surrogate model convergence factor a

Output: Probabilistic response data $\mathbf{\Theta}$, Posterior distribution $P(\theta|\mathbf{V})$, Surrogate model $\hat{f}$

$inc = inc_0$
$conv = a + 1$
$i = 0$
while $conv > a$ **do**
  $i = i + 1$
  $\mathbf{X}^{inc} = LHS(P(\theta), inc)$
  $\mathbf{Y}^{inc} = f(\mathbf{X}^{inc})$ {High fidelity model}
  $\hat{f}_i = Train(\mathbf{X}, \mathbf{Y})$ {Construct low fidelity model through data driven method}
  $A^i = AccuracyCheck(\hat{f}_i)$
  if $i \geq 2$ **then**
    $conv = |A^i - A^{i-1}|$
  end if
  $inc = inc + inc_0$
end while
$\hat{f} = \hat{f}_i$
$P(\theta|\mathbf{V}) = BMU(P(\theta), \mathbf{V}, \sigma_p, \hat{f})$
$\theta = MCS(P(\theta|\mathbf{V}))$ {Draw samples from posterior distribution through Monte-Carlo simulations}
$\mathbf{\Theta} = \hat{f}(\theta)$

Beginning with level 2 this gives models a starting base of data and reduces the number of times the costly high fidelity model is run. Once each layer is complete the final data-driven model and posterior distribution are saved and used to generate final probabilistic response data.

III. Case study

In this section the nonlinear aeroelatic test case is presented. First the experimental setup will be described followed by the employed mathematical model. Application of the multilevel process to the test case is then laid out. Finally results from both single- and multilevel data-driven updating are shown and compared.

Figure 2a shows the experimental flutter rig comprised of a NACA-0015 wing profile rigidly attached to a stainless steel shaft. The aerofoil is supported by rotational bearings on each end allowing for rotation and a bearing system allowing vertical displacement. The spring in the heave degree of freedom behaves in a linear manner. In the bearings, leaf springs are introduced to create a nonlinear hardening effect in pitch motion. Airspeed in the wind tunnel was increased and amplitude data for LCO was gathered. Data was collected using control-based continuation (CBC), providing access to both stable and unstable responses of the system (see [33] for more explanations about CBC and its exploitation in this context). Experimental points are shown in Figure 3, where subcritcal behaviour is observed. Further detail on the experiment is found in [33].

The flutter rig is modelled as the two-degree-of-freedom system shown in Figure 2b coupled with an unsteady aerodynamic model described by Abdelkef et al. [34]. The mathematical model takes the form of the standard nonlinear aeroelastic equation

$$\mathbf{M}\ddot{x} + \mathbf{D}\dot{x} + \mathbf{K}x + q_{nl}f_{nl} = \mathbf{A}(\rho)\ddot{x} + \mathbf{B}(\rho V)\dot{x} + \mathbf{C}(\rho V^2)x \tag{3}$$

Where x denotes the system's degrees of freedom and $\mathbf{M}$,$\mathbf{D}$ and $\mathbf{K}$ are the structural mass, damping and stiffness matrices respectively. Matrices $\mathbf{A}$ $\mathbf{B}$ and $\mathbf{C}$ are aerodynamic matrices which are dependent on air density and freestream velocity. All matrices are size $N \times N$ where N is the number of degrees of freedom of the system. The nonlinear function f_{nl} is used to represent different types of nonlinearities encountered in aeroelastic systems. The $N \times 1$ vector q_{nl} is utilised to implement the nonlinear equations in the degrees of freedom they impact. The content and parameter values of each matrix is laid out in [21]. For this study the assumed spring stiffness is approximated by quadratic and cubic terms in pitch degree of freedom (which is typically used to represent geometrical nonlinearities):

$$f_{nl} = K_{\alpha 2}\alpha^2 + K_{\alpha 3}\alpha^3 \tag{4}$$

Algorithm 2 Multi-level data-driven BMU

Input: Experimental data $\mathbf{V}$, Initial prior distribution $P(\theta)^0$, Number of levels N_{level}, Width parameter σ_p, Training data increment inc_0, Surrogate model convergence factor a

Output: Probabilistic response data $\mathbf{\Theta}$, Final posterior distribution $P(\theta|\mathbf{V})$, Final surrogate model $\hat{f}$

Initialization $P(\theta)^1 = P(\theta)^0$
$n = 0$
while $n \leq N_{level}$ **do**
  $n = n + 1$
  $\sigma_p^n = \sigma_p * (N_{level} + 1 - n)$
  $inc = inc_0$
  $conv = a + 1$
  $i = 0$
  while $conv > a$ **do**
    $i = i + 1$
    $\mathbf{X}^{inc} = LHS(P(\theta)^n, inc)$
    $\mathbf{Y}^{inc} = f(\mathbf{X}^{inc})$ {Samples already in data base are not rerun}
    $\hat{f}_i = Train(\mathbf{X}, \mathbf{Y})$
    $A^i = AccuracyCheck(\hat{f}_i)$
    if $i \geq 2$ **then**
      $conv = |A^i - A^{i-1}|$
    end if
    $inc = inc + inc_0$
  end while
  $\hat{f}_n = \hat{f}_i$ {Converged surrogate model at n^{th} layer}
  $P(\theta|\mathbf{V})^n = BMU(P(\theta)^n, \mathbf{V}, \sigma_p^n, \hat{f}_n)$
  $P(\theta)^{n+1} = P(\theta|\mathbf{V})^n$ {Define prior for next level as posterior of previous layer}
  $[\mathbf{X}, \mathbf{Y}] = DiscardData(P(\theta|\mathbf{V})^n, [\mathbf{X}, \mathbf{Y}])$ {Discard data from training data base that is not within n^{th} prior distribution}
end while
$P(\theta|\mathbf{V}) = P(\theta)^{n+1}$
$\hat{f} = \hat{f}_{n-1}$
$\theta = MCS(P(\theta|\mathbf{V}))$
$\mathbf{\Theta} = \hat{f}(\theta)$

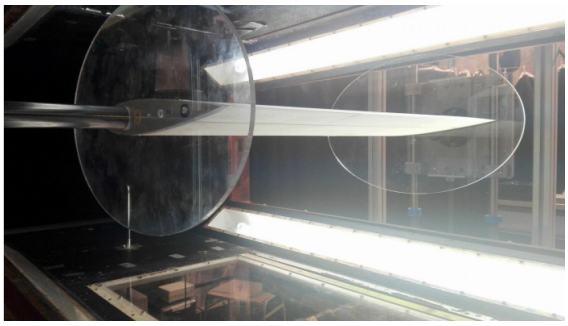

(a) Experimental configuration [33]

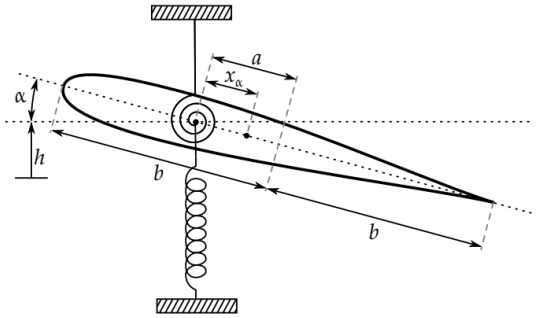

(b) 2 DOF Freebody diagram

Fig. 2 Nonlinear flutter test rig

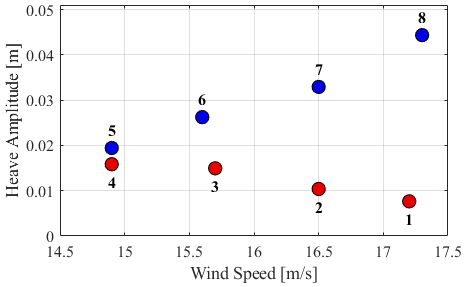

Fig. 3 Labelled experimental data (• stable LCO) (• unstable LCO)

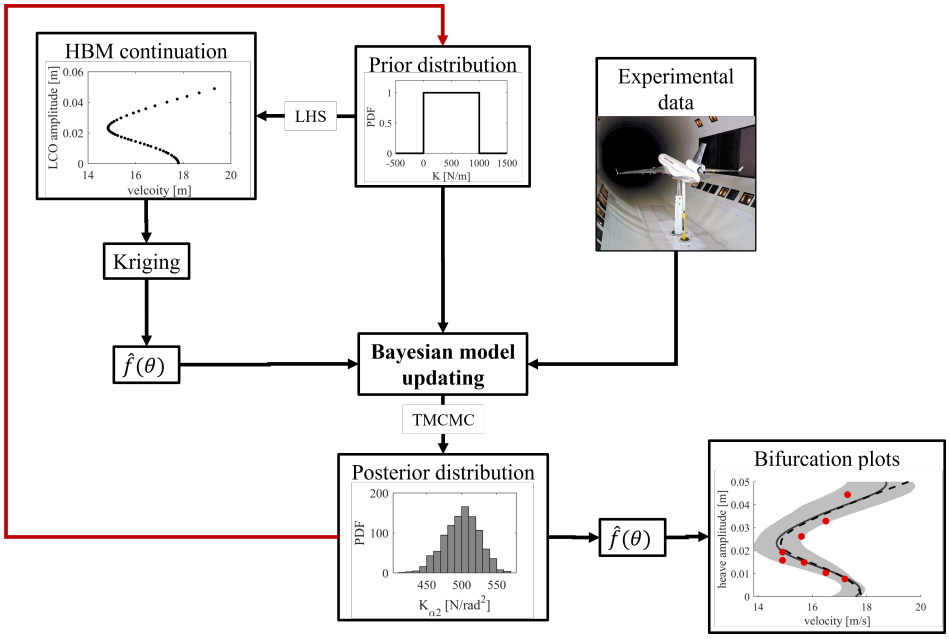

Fig. 4 Multilevel data-driven BMU applied to nonlinear aeroelastic case

Nonlinear parameters $K_{\alpha 2}$ and $K_{\alpha 3}$ are treated as unknowns. The methodology described in this paper will work to estimate the nonlinear parameters with the described processes. The flowchart in Figure 4 details how the data driven multilevel updating is applied to the aeroelastic test case. Presence of the highlighted feedback loop is the key difference between the sing- and multilevel process. High fidelity model f is a Harmonic Balance (HBM) continuation process [9, 35]. Based on inputs $K_{\alpha 2}$ and $K_{\alpha 3}$, a bifurcation diagram is produced with data for velocity and LCO heave amplitude output. Even with this low degree of freedom case study, this process can take between 3-10 seconds. A Kriging algorithm is used to train data-driven model $\hat{f}$ [36]. To effectively capture subcritical behaviour, $\hat{f}$ is set up with $K_{\alpha 2}$, $K_{\alpha 3}$ and LCO amplitude as inputs and velocity as the output. This set up allows the subcritcal behaviour to be effectively recreated as only unique pairings of $K_{\alpha 2}$, $K_{\alpha 3}$ and LCO amplitude should exist in the training data. Further detail on this process can be found in previous studies where the single-level approach is applied [21].

A. Single-level

The single-level process is applied to the case study and results are presented here as a reference case for the multilevel study. Inputs to the algorithm are displayed in Table 1. Prior distributions $P(\theta)$ for each parameter is taken to be uniform within the defined boundaries. Based on prior knowledge and experiments, the magnitude of quadratic stiffness should not exceed $1e^3[N/rad^2]$ and for cubic stiffness $1e^4[N/rad^3]$. It is possible however for parameters to be both positive and negative. Width parameter was determined based on experiments with the converged surrogate model. Bayesian model updating with TMCMC sampling is carried out until acceptance rate is as close to the idea

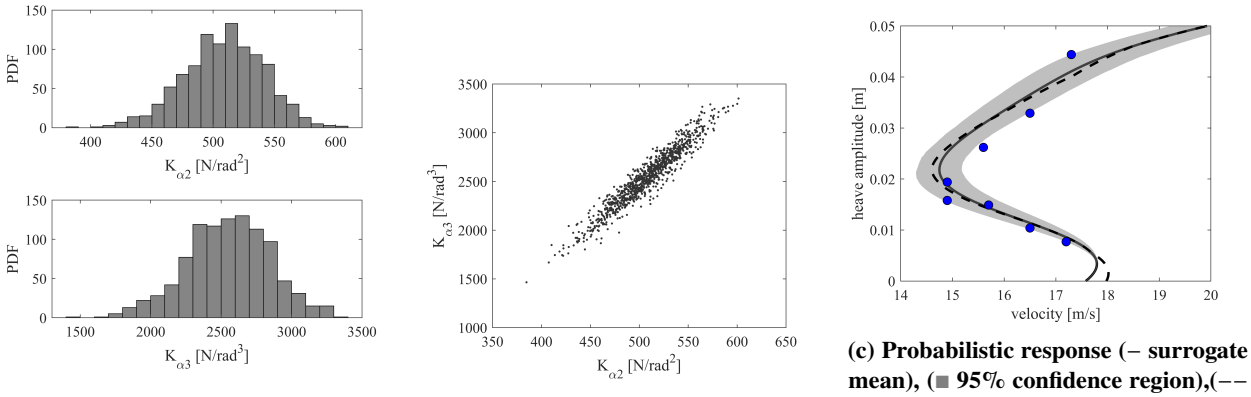

(a) Nonlinear parameter histograms **(b) TMCMC scatter plot** **(c) Probabilistic response (− surrogate mean), (■ 95% confidence region),(−− HBM continuation), (• CBC data)**

Fig. 5 Single-level data-driven BMU probabilistic parameters and response

Table 1 Single-level data-driven BMU inputs and outputs

inputs				outputs				
$P(\theta)$	σ_p	inc_0	a	mean	COV	$\hat{f}$ accuracy	f runs	$\hat{f}$ runs
$K_{\alpha 2}$: Uniform(-1e^3, 1e^3)	0.6	10	0.5%	$K_{\alpha 2}$: 508.6N/rad^2	6.43%	96.7%	1200	2000
$K_{\alpha 3}$: Uniform(-1e^4, 1e^4)	-	-	-	$K_{\alpha 3}$: 2549.9N/rad^3	11.68%	-	-	-

value of 0.234 as possible.

In constructing a single surrogate model spanning the whole design space, accuracy is found to converge at 75%. This is deemed too large an error to extract meaningful results from in the single-level process. It is theorised the low accuracy is a result of the large amount of varied behaviour between different combinations of positive and negative inputs for nonlinear parameters. To resolve this, the design space is divided into four sub design spaces based on the sign of each nonlinear stiffness parameter. As there is two input parameters this results in +/+, +/-, -/+ and -/- regions. Separate data-driven models are built and linked into a full model with an "if" statement. This is similar to the method used in the previous study [21]. Accuracy of the segmented model converges at 96.7% with 1200 training samples in total.

With TMCMC, 1000 samples are drawn from the data-driven model to ensure a stationary solution was reached. A further 1000 samples are drawn via MCS from $\hat{f}$ to determine probabilistic behaviour. The data-driven model takes on average 0.0012 seconds to run. The results are displayed in Figure 5 and Table 1. Histograms with normal shapes are produced, with relatively low coefficient of variance (COV) suggesting a single-modal solution. The bifurcation diagram produced captures a majority of the behaviour within the confidence bands. Using mean parameter estimates directly with HBM continuation produces results that slightly deviate from the surrogate model mean. Particularly at low amplitude points close to the hopf bifurcation. This leaves room for improvement in accuracy of the final Kriging model. These results are used as a reference point for the multilevel study.

B. Multilevel

The multilevel process is now applied to the case study. Results are presented then compared to the single-level results. Inputs into the algorithm are shown in Table 2. Initial prior distributions are the same as the prior distributions from the single-level study. Final width parameter also remains the same so results can be compared effectively. Accuracy convergence criterion of the data-driven model is increased from 0.5% to 2% to allow for coarser models at lower levels. In this study, the number of levels was set to three.

Figure 6 displays the evolution of the process at each level. All training data at each level is shown, and the TMCMC scatter plots generated using the resulting data-driven models is presented. It can be observed, that the algorithm effectively updates the design space based on the current model and uses the updated prior to gather refined training

Table 2 Multilevel data-driven BMU inputs and outputs

inputs					outputs				
$P(\theta)^0$	N	σ_p	inc_0	a	mean	COV	$\hat{f}$ accuracy	f runs	$\hat{f}$ runs
$K_{\alpha 2}$: Uniform(-1e^3, 1e^3)	3	0.6	10	2%	$K_{\alpha 2}$: 499.9N/rad^2	5.0%	99.8%	309	4000
$K_{\alpha 3}$: Uniform(-1e^4, 1e^4)	-	-	-	-	$K_{\alpha 3}$: 2356.6N/rad^3	8.3%	-	-	-

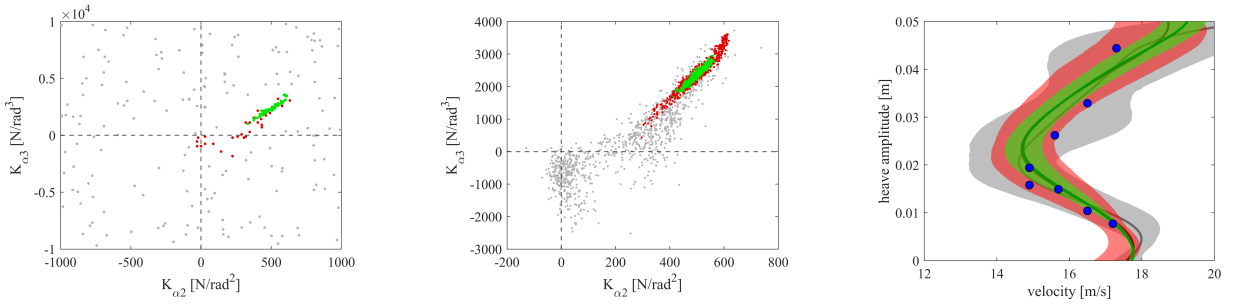

(a) training data **(b) TMCMC scatter plot** **(c) Probabilistic bifurcation diagrams**

Fig. 6 Level comparison (● level 1),(● level 2),(● level 3)

data. It is apparent the process has converged to a single modal solution. Evolution of the probabilistic response is displayed in Figure 6c with shaded areas representing 95% confidence regions. The response at level 1 is chaotic. The mean response of level 2 and 3 is almost identical but with a noticeable increase in confidence between the levels.

Figures 7 and 8 describe the process through which training data is gathered for each data-driven model. The shaded area in Figure 8 is based on the prior distribution from model updating shown in Figures 7b and 7c. Data within the shaded area is saved and used in construction of the next model. Figure 9 shows the accuracy convergence of each data-driven model. Average accuracy of the model improves by up to 30% between level 1 and 2. The final surrogate model converges close to 100%.

Final results of the process are summarised in Figure 10 and Table 2. The shape of the histogram and the scatter plot is close to the final result of the single-level result. The probabilistic response takes a slightly different shape, capturing less of the data within the confidence region. The mean plot from the data-driven model is in closer agreement with the plot directly from HBM continuation than in the single-level study. This suggest greater confidence can be placed in the results. With reference to Tables 1 and 2, final result for mean $K_{\alpha 2}$ and $K_{\alpha 3}$ are within 2% of the single-level results but with lower COV. Table 3 breaks down the multilevel results form each level. The change mean between level 2 and 3 is less than 1% but there is a noticeable reduction in COV and data-driven model accuracy. The result of this is on the probabilistic response can be seen in Figure 6c. Accuracy of the level 3 model offers an improvement over

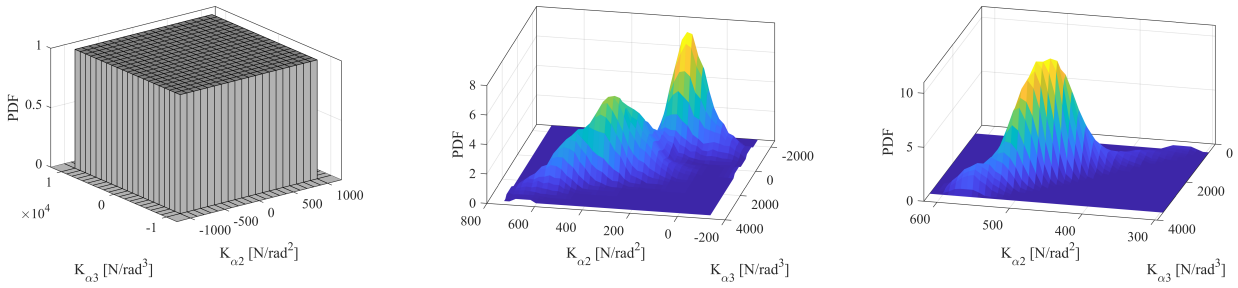

(a) Level 1 **(b) Level 2** **(c) Level 3**

Fig. 7 Prior distributions at each level

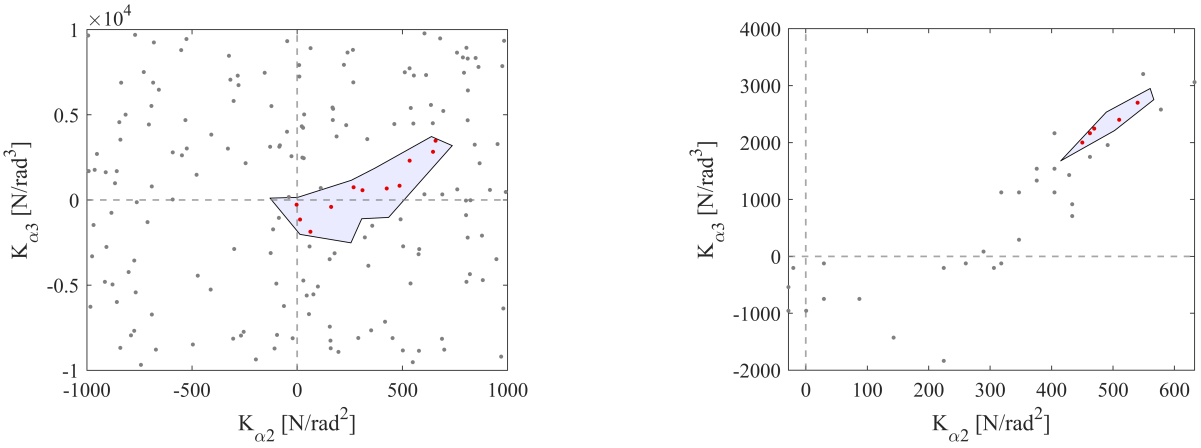

(a) Level 1 to 2 **(b) Level 2 to 3**

Fig. 8 Training data selection (● discarded data),(● saved data)

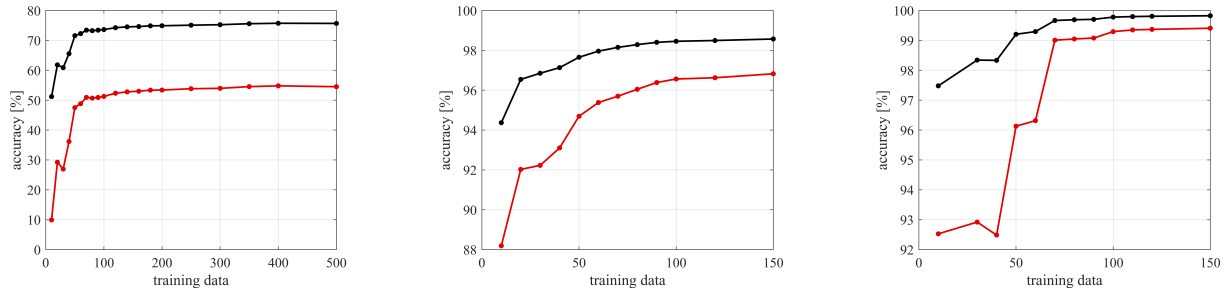

(a) Level 1 **(b) Level 2** **(c) Level 3**

Fig. 9 Accuracy of data-driven model at each level (– mean accuracy),(– –std accuracy)

Table 3 Progression of results at each level

Level	mean $K_{\alpha 2}$	COV $K_{\alpha 2}$	mean $K_{\alpha 3}$	COV $K_{\alpha 3}$	Surrogate accuracy	f runs
1	$235.6 N/rad^2$	79.9%	$345.7 N/rad^3$	338.8%	74.9%	180
2	$497.3 N/rad^2$	11.6%	$2356.9 N/rad^3$	20.6%	97.1%	40(+29)
3	$499.9 N/rad^2$	5.0%	$2356.6 N/rad^3$	8.3%	99.8 %	100(+95)

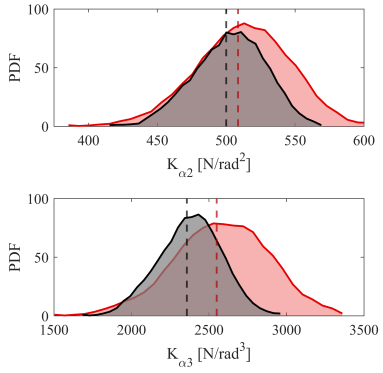

(a) Nonlinear parameter histogram (−− mean line)

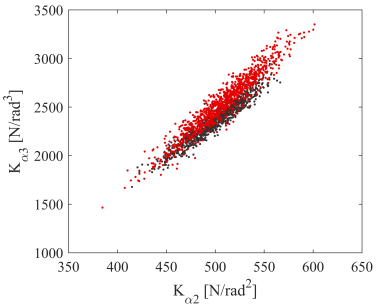

(b) TMCMC scatter plot

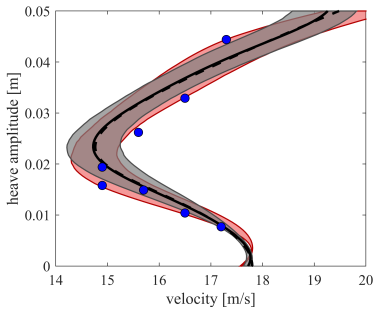

(c) Probabilistic response (− surrogate mean), (■ 95% confidence region),(−− HBM continuation), (• CBC data)

Fig. 10 Multilevel data-driven BMU probabilistic parameters and response (• Multilevel),(• Single-level)

the 96.7% accurate model in the single-level study. Level 2 model is also more accurate than the single-level model. Training data requirement is the key area where the largest disparity is observed. Despite the model construction taking 40 input runs at level 2, 11 points from the 180 gathered in the level 1 are within the shaded area in Figure 8a. So only 29 additional training points are required. Similarly at level 3, 5 points from the previous level's data collection are within the design space. This results in a total training data requirement of 309 input continuation runs. That is a 74% reduction on the 1200 samples required in the single-level study. The data-driven model is run 1000 times at each level and 1000 further times to determine probabilistic behaviour. Average time to run f is 6.5s and $\hat{f}$ is 0.0012s. This gives a total run time of 2.17 hours for single-level and 33.56 minutes for multilevel. Potential run time is reduced also by 74% in the multilevel study. Neither the single or multilevel process perfectly capture the behaviour of the experimental data, both producing similar results. The difference between the prediction and experimental results is likely down to the choice of a low-degree of freedom model or character of the nonlinearity.

IV. Conclusion

The results of this study have demonstrated that the proposed multilevel data-driven approach can both significantly reduce training data requirements and improve surrogate accuracy compared to the single-level approach through Bayseian model updating. Using the nonlinear aerofoil aeroelatic test case, nonlinear parameters were stochastically identified with single- and multilevel approaches and compared. The proposed multilevel approach offered a 74% reduction in training data requirements/run time and 3% increase in data-driven model accuracy whilst producing parameter estimates within 2% of that from single-level BMU study. However, neither study fully capture the LCO behaviour observed in the experimental data, suggesting the mathematical model could be improved further. Taking forward the promising results from this study, the full benefits of the multilevel approach should be demonstrated on a high fidelity aeroelastic test case. Further work should also be conducted on determining accuracy criterion of the coarse data-driven models, with the goal of reducing training data requirements further.

	Single-level	Multilevel
mean $K_{\alpha 2}$ $[N/rad^2]$	508.6	499.9
COV $K_{\alpha 2}$ [%]	6.4	5.0
mean $K_{\alpha 3}$ $[N/rad^3]$	2549.9	2356.6
COV $K_{\alpha 3}$ [%]	11.7	8.3
$\hat{f}$ accuracy [%]	96.7	99.8
f runs	1200	309
$\hat{f}$ runs	2000	4000
run time [mins]	130.2	33.6

Table 4 Caption

Acknowledgements

M. McGurk acknowledge the support from the EPSRC Doctoral Training Partnership (DTP) studentship for his PhD study at the University of Strathclyde. J.Yuan also acknowledges the funding support of the Royal Academy of Engineering/Leverhulme Trust Research Fellowship (LTRF2223-19-150).

Data acknowledgement

The authors acknowledge the work of experiemntal work by Kyoung Hyun Lee. Experimental data is available at `https://github.com/Kyounghyunlee/`

References

[1] Dimitriadis, G., *Introduction to nonlinear aeroelasticity*, John Wiley & Sons, 2017.

[2] Ghaffari, R., and Sauer, R. A., "Modal analysis of graphene-based structures for large deformations, contact and material nonlinearities," *Journal of Sound and Vibration*, Vol. 423, 2018, pp. 161–179. https://doi.org/https://doi.org/10.1016/j.jsv.2018.02.051, URL https://www.sciencedirect.com/science/article/pii/S0022460X18301470.

[3] Shukla, H., and Patil, M. J., "Nonlinear state feedback control design to eliminate subcritical limit cycle oscillations in aeroelastic systems," *Nonlinear Dynamics*, Vol. 88, 2017, pp. 1599–1614.

[4] Guckenheimer, J., and Holmes, P., *Nonlinear oscillations, dynamical systems, and bifurcations of vector fields*, Vol. 42, Springer Science & Business Media, 2013.

[5] Tang, D., and Dowell, E. H., "Experimental and theoretical study on aeroelastic response of high-aspect-ratio wings," *AIAA journal*, Vol. 39, No. 8, 2001, pp. 1430–1441.

[6] Patil, M. J., Hodges, D. H., and Cesnik, C. E., "Limit-cycle oscillations in high-aspect-ratio wings," *Journal of fluids and structures*, Vol. 15, No. 1, 2001, pp. 107–132.

[7] Avin, O., Raveh, D. E., Drachinsky, A., Ben-Shmuel, Y., and Tur, M., "An experimental benchmark of a very flexiblewing," *AIAA Scitech 2021 Forum*, 2021, p. 1709.

[8] Drachinsky, A., Avin, O., Raveh, D. E., Ben-Shmuel, Y., and Tur, M., "Flutter tests of the Pazy wing," *AIAA Journal*, Vol. 60, No. 9, 2022, pp. 5414–5421.

[9] McGurk, M., and Yuan, J., "Computation of limit cycle oscillations and their stabilities in nonlinear aeroelastic systems using harmonic balance methods," *Proceedings of the International Forum on Aeroelasticity and Structural Dynamics*, Madrid, 2022.

[10] Beregi, S., Barton, D. A., Rezgui, D., and Neild, S., "Using scientific machine learning for experimental bifurcation analysis of dynamic systems," *Mechanical Systems and Signal Processing*, Vol. 184, 2023, p. 109649. https://doi.org/https://doi.org/10.1016/j.ymssp.2022.109649, URL https://www.sciencedirect.com/science/article/pii/S0888327022007348.

[11] Stolovitch, L., "Progress in normal form theory," *Nonlinearity*, Vol. 22, No. 7, 2009, p. R77.

[12] Kaba, A., Metin, E. Y., and Turan, O., "Thrust modelling of a target drone engine with nonlinear least–squares estimation based on series expansions," *Aircraft Engineering and Aerospace Technology*, , No. ahead-of-print, 2022.

[13] Eiselt, H., Sandblom, C.-L., et al., *Nonlinear optimization*, Springer, 2019.

[14] Friswell, M., and Mottershead, J. E., *Finite element model updating in structural dynamics*, Vol. 38, Springer Science & Business Media, 1995.

[15] Bi, S., Beer, M., Cogan, S., and Mottershead, J., "Stochastic Model Updating with Uncertainty Quantification: An Overview and Tutorial," *Mechanical Systems and Signal Processing*, Vol. 204, 2023, p. 110784.

[16] Beck, J. L., and Katafygiotis, L. S., "Updating models and their uncertainties. I: Bayesian statistical framework," *Journal of Engineering Mechanics*, Vol. 124, No. 4, 1998, pp. 455–461.

[17] Namdeo, V., and Manohar, C., "Nonlinear structural dynamical system identification using adaptive particle filters," *Journal of Sound and Vibration*, Vol. 306, No. 3-5, 2007, pp. 524–563.

[18] Green, P. L., and Worden, K., "Bayesian and Markov chain Monte Carlo methods for identifying nonlinear systems in the presence of uncertainty," *Philosophical Transactions of the Royal Society A: Mathematical, Physical and Engineering Sciences*, Vol. 373, No. 2051, 2015, p. 20140405.

[19] Ebrahimian, H., Astroza, R., and Conte, J. P., "Extended Kalman filter for material parameter estimation in nonlinear structural finite element models using direct differentiation method," *Earthquake Engineering & Structural Dynamics*, Vol. 44, No. 10, 2015, pp. 1495–1522.

[20] Yin, M., Iannelli, A., and Smith, R. S., "Maximum likelihood estimation in data-driven modeling and control," *IEEE Transactions on Automatic Control*, 2021.

[21] McGurk, M., Lye, A., Renson, L., and Yuan, J., "Data-driven Bayesian inference for stochastic model identification of nonlinear aeroelastic systems," *AIAA Journal*, Vol. pre-print, 2023.

[22] Barton, D. A., Mann, B. P., and Burrow, S. G., "Control-based continuation for investigating nonlinear experiments," *Journal of Vibration and Control*, Vol. 18, No. 4, 2012, pp. 509–520.

[23] Saltari, F., Traini, A., Gambioli, F., and Mastroddi, F., "A linearized reduced-order model approach for sloshing to be used for aerospace design," *Aerospace Science and Technology*, Vol. 108, 2021, p. 106369.

[24] Kou, J., and Zhang, W., "Layered reduced-order models for nonlinear aerodynamics and aeroelasticity," *Journal of Fluids and Structures*, Vol. 68, 2017, pp. 174–193.

[25] Thomas, P. V., ElSayed, M. S., and Walch, D., "Review of model order reduction methods and their applications in aeroelasticity loads analysis for design optimization of complex airframes," *Journal of Aerospace Engineering*, Vol. 32, No. 2, 2019, p. 04018156.

[26] Guo, M., McQuarrie, S. A., and Willcox, K. E., "Bayesian operator inference for data-driven reduced-order modeling," *Computer Methods in Applied Mechanics and Engineering*, Vol. 402, 2022, p. 115336.

[27] Prudhomme, S., and Bryant, C. M., "Adaptive surrogate modeling for response surface approximations with application to bayesian inference," *Advanced Modeling and Simulation in Engineering Sciences*, Vol. 2, No. 1, 2015, pp. 1–21.

[28] Detommaso, G., Dodwell, T., and Scheichl, R., "Continuous level Monte Carlo and sample-adaptive model hierarchies," *SIAM/ASA Journal on Uncertainty Quantification*, Vol. 7, No. 1, 2019, pp. 93–116.

[29] Dodwell, T. J., Ketelsen, C., Scheichl, R., and Teckentrup, A. L., "Multilevel markov chain monte carlo," *Siam Review*, Vol. 61, No. 3, 2019, pp. 509–545.

[30] Lye, A., Cicirello, A., and Patelli, E., "Sampling methods for solving Bayesian model updating problems: A tutorial," *Mechanical Systems and Signal Processing*, Vol. 159, 2021, p. 107760. https://doi.org/https://doi.org/10.1016/j.ymssp.2021.107760, URL https://www.sciencedirect.com/science/article/pii/S0888327021001552.

[31] Roberts, G. O., and Rosenthal, J. S., "Optimal scaling for various Metropolis-Hastings algorithms," *Statistical science*, Vol. 16, No. 4, 2001, pp. 351–367.

[32] Gelman, A., Gilks, W. R., and Roberts, G. O., "Weak convergence and optimal scaling of random walk Metropolis algorithms," *The annals of applied probability*, Vol. 7, No. 1, 1997, pp. 110–120.

[33] Lee, K., Barton, D., and Renson, L., "Model identification of a fluttering aerofoil using control-based continuation and normal form analysis," *Proceedings of the International Conference on Noise and Vibration Engineering, ISMA*, 2020, pp. 261–268.

[34] Abdelkefi, A., Vasconcellos, R., Nayfeh, A. H., and Hajj, M. R., "An analytical and experimental investigation into limit-cycle oscillations of an aeroelastic system," *Nonlinear Dynamics*, Vol. 71, No. 1, 2013, pp. 159–173.

[35] Detroux, T., Renson, L., Masset, L., and Kerschen, G., "The harmonic balance method for bifurcation analysis of large-scale nonlinear mechanical systems," *Computer Methods in Applied Mechanics and Engineering*, Vol. 296, 2015, pp. 18–38.

[36] Sun, Y., Denimal, E., Yuan, J., and Salles, L., "Geometric design of friction ring dampers in blisks using nonlinear modal analysis and Kriging surrogate model," *Structural and Multidisciplinary Optimization*, Vol. 65, No. 3, 2022, p. 98.